Nanoscale Res Lett (2009) 4:1512–1516
DOI 10.1007/s11671-009-9428-1

NANO EXPRESS

Synthesis of Novel Flower-Like Zn(OH)F via a Microwave-Assisted Ionic Liquid Route and Transformation into Nanoporous ZnO by Heat Treatment

Jia-kui Song · Ming-bo Zheng · Zhen-jiang Yang · Hui-qin Chen · Hai-yan Wang · Jin-song Liu · Guang-bin Ji · Hai-qian Zhang · Jie-ming Cao

Received: 15 June 2009 / Accepted: 19 August 2009 / Published online: 16 September 2009

Abstract Zinc hydroxide fluoride (Zn(OH)F) with novel flower-like morphology has been prepared via a microwave-assisted ionic liquid route. The flower-like Zn(OH)F particle has six petals and every petal is composed of lots of acicular nano-structure. Nanoporous ZnO is obtained by thermal decomposition of as-prepared Zn(OH)F in air, and the flower-like morphology is well retained. In the process of synthesis, ionic liquid 1-Butyl-3-methylimidazolium tetrafluoroborate is used as both the reactant and the template.

Keywords Ionic liquid · Microwave · Zn(OH)F · Nanoporous ZnO · Flower-like

Introduction

The conventional inorganic synthetic procedures usually demand long reaction time, high temperature, and toxic solvents. Different from the traditional solvents, ionic liquids are potential green solvents with many advantages, such as negligible vapor pressure, low interface tension, supramolecular solvents, and microwave absorbing ability [1, 2]. Because of these excellent performances, ionic liquids can be the new "all in one" solvents, which are combination of solvent, template, and reactant [3]. Compared with the traditional heating methods, microwave irradiation can obviously shorten the heating time. Moreover, microwave irradiation also has many other advantages, including volumetric heating, selectivity, fast kinetics, homogeneity, and energy saving [4–9]. Microwave-assisted ionic liquid reaction systems have been studied for the synthesis of inorganic materials, such as ZnO frameworks [10], high quality TiO_2 nanocrystals [11], Bi_2Se_3 nanosheets [4], indium tin oxide nanocrystals [12], metal fluorides [13], cuboid-like crystallites [14], tellurium nanorods and nanowires [15], manganese oxide [16], CdF_2 nanoflakes [17], and ZnO nanosheet aggregates [18].

Zn(OH)F has been demonstrated to be an important catalyst for the formation of pyridine from tetrahydrofurfuryl alcohol and ammonia, and it has also been used as the precursor for preparing ZnO [19, 20]. Huang et al. [20] have presented a simple hydrothermal route toward Zn(OH)F, which was then used as the precursor to prepare ZnO by calcination. As we know, ZnO has a wide range of applications in gas sensors, piezoelectric transducers, optical waveguides, acoustic–optical devices, catalysis, and solar cells, mainly due to its unique catalytic, electronical, and optoelectric properties [21–23]. Recently, porous ZnO with large specific surface area has generated considerable interest because of its potential applications in photocatalysis, environmental engineering to chemical, and gas sensors [24, 25]. Porous ZnO with various nanostructures have been reported, including hollow ZnO mesocrystals [26], porous ZnO nanoparticles [24], porous ZnO architectures [25], porous ZnO nanodisks [27], and porous ZnO nanowires [28].

Herein, for the first time, ionic liquid 1-Butyl-3-methylimidazolium tetrafluoroborate ($[Bmim]BF_4$) is used as the reactant and the template to synthesize novel flower-like Zn(OH)F via an easy and fast microwave-assisted route. Nanoporous ZnO is obtained by thermal decomposition of the Zn(OH)F.

J. Song · M. Zheng · Z. Yang · H. Chen · H. Wang · J. Liu · G. Ji · H. Zhang · J. Cao (✉)
Nanomaterials Research Institute, College of Materials Science and Technology, Nanjing University of Aeronautics and Astronautics, Nanjing 210016, China
e-mail: jmcao@nuaa.edu.cn

Experimental Section

All reagents are of analytical grade and used without further purification. In a typical synthesis, 0.22 g (1 mmol) of $Zn(CH_3COO)_2{\cdot}2H_2O$ powder was dissolved in 8 mL of distilled water under stirring at room temperature for 10 min, then 2 mL of $[Bmim]BF_4$ was added slowly while the stirring continued. Afterward, the mixture was transferred to a 30 mL Teflon-liner tube and kept inside a domestic microwave oven for 5 min (800 W, 40% of maximum power). The obtained white precipitate was washed with distilled water and pure ethanol and collected by centrifugation. The collected Zn(OH)F sample was dried at 60 °C in vacuum for 12 h. Then, the Zn(OH)F sample was calcined at 400 °C for 2 h in air atmosphere, to yield final product ZnO.

The obtained samples were characterized by X-ray diffraction (XRD) (Bruker D8 advance), field-emission scanning electron microscopy (FESEM) (LEO 1530), transmission electron microscopy (TEM) (JEOL JEM-2100), and nitrogen adsorption–desorption analysis (Micromeritics ASAP2010).

Results

Figure 1a shows the XRD pattern of the product of microwave reaction. The XRD pattern reveals that the main composition of the product is Zn(OH)F (JCPDS 32-1469) and a few impurities can also be detected. As shown in Fig. 1a, the peaks corresponding to Zn(OH)F are identified. Figure 1b shows the XRD pattern of the product after the heat treatment, and the pattern matches well with the standard pattern of ZnO (JCPDS 36-1451). No impurity peaks are detected indicating the high purity of the ZnO phase.

SEM images of Zn(OH)F are shown in Fig. 2a–c. The SEM images reveal that the sample is composed of regular hierarchical flower-like particles and the average size of the flower-like particles is about 7 μm. All the flower-like particles have six petals and every petal is composed of lots of acicular nano-structures, which grow from the center to the edge. The average length of each petal is about 3 μm. The magnified image of a typical petal is shown in Fig. 2c.

Figure 2d–f shows the SEM images of ZnO sample. The images reveal that the ZnO sample retains the flower-like morphology after the heat treatment at 400 °C. The size of the ZnO particles is similar to that of the precursor Zn(OH)F. The magnified image (Fig. 2f) indicates that ZnO sample possesses nanoporous structure.

Figure 3 shows the TEM images of the precursor Zn(OH)F and the corresponding ZnO. Figure 3a gives the micrograph of a typical Zn(OH)F petal and the selected area electron diffraction (SAED) pattern of the circular area. The SAED pattern indicates the acicular nano-structure possesses single crystal structure. Besides, Fig. 3a reveals that the petal of the flower-like particle does not have porous structure. After the heat treatment, the ZnO sample exhibits nanoporous structure, as shown in Fig. 3b. The SAED pattern reveals that the petal of the particle possesses quasi-single crystal structure. The high-resolution transmission electron microscopy (HRTEM) images for the petal are presented in Fig. 3c and d. Figure 3d shows the lattice fringes, whose spacing is 0.2476 nm, which is corresponding to the *d* value of the (101) planes of ZnO.

Figure 4 shows the nitrogen adsorption–desorption isotherm and the pore size distribution plot of nanoporous ZnO. The isotherm is identified as type IV, which is corresponding to the characteristic of mesoporous materials. The BET surface area of the porous ZnO is about 38.2 m^2/g, which is obviously larger than that of commercial ZnO powder with a BET surface area of ca. 4–5 m^2/g [26]. BJH pore size distribution plot (Fig. 4b) shows a broad peak in a region of 5–50 nm with an obvious maximum at about 17 nm.

Discussion

Based on the experimental results, it can be confirmed that the addition of ionic liquids and the microwave irradiation play important roles in the formation of Zn(OH)F with

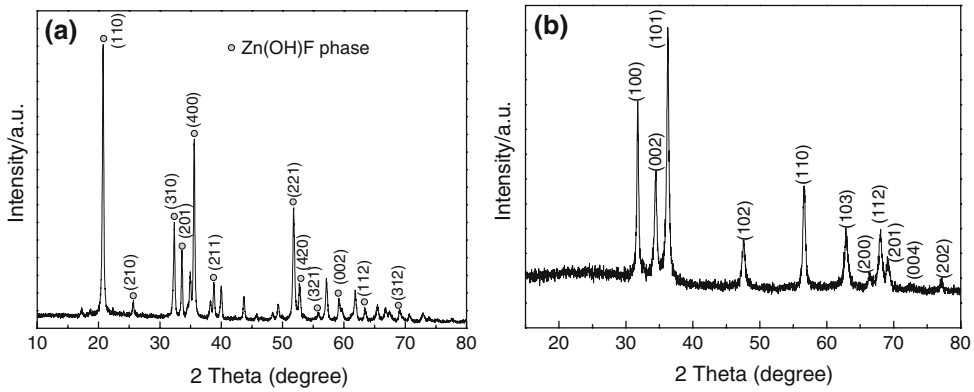

Fig. 1 **a** XRD pattern of as-prepared Zn(OH)F, **b** XRD pattern of ZnO

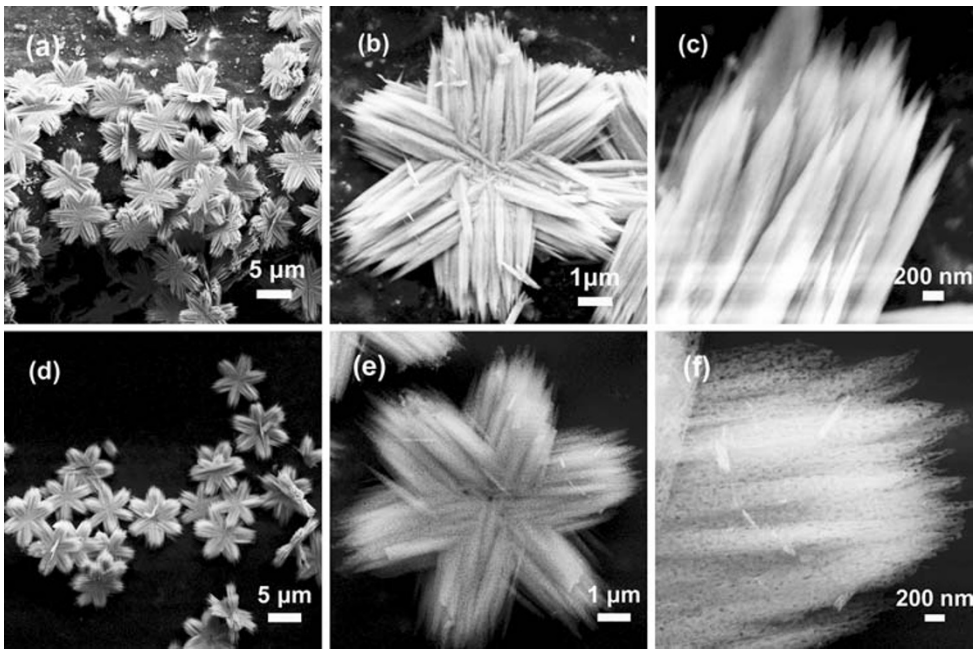

Fig. 2 **a**–**c** SEM images of as-prepared Zn(OH)F, **d**–**f** SEM images of nanoporous ZnO

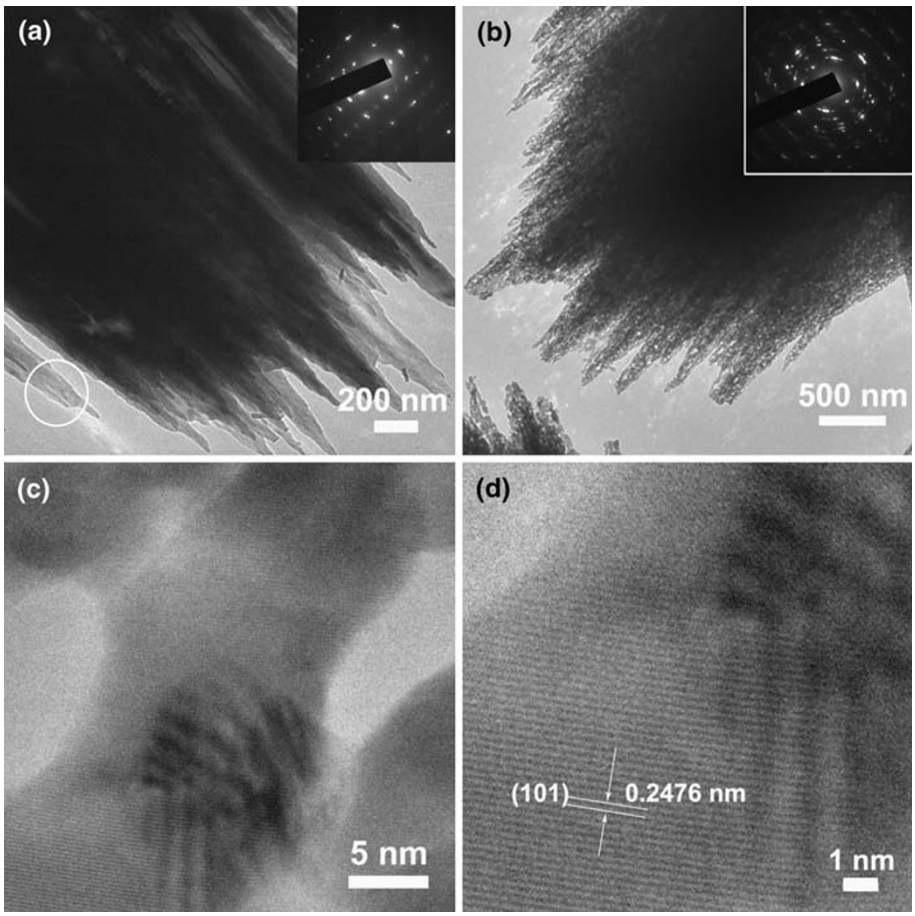

Fig. 3 **a** TEM images of the precursor Zn(OH)F and electron diffraction pattern of Zn(OH)F (insert **a**, corresponding to the circle area of panel **a**), **b** TEM images of ZnO and electron diffraction pattern (insert **b**), and **c**, **d** HRTEM images of ZnO

novel structure. First, microwave is one kind of electromagnetic energy. It can obviously shorten the heating time and increase the heating efficiency. Second, because ionic liquids are composed of inorganic anion and organic cation, they have high polarizability and conductivity. The ionic nature makes ionic liquid good solvent for absorbing

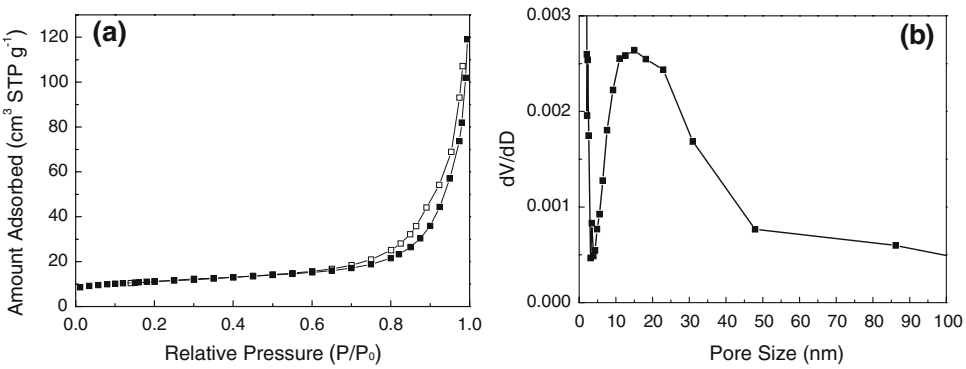

Fig. 4 **a** Nitrogen adsorption–desorption isotherm for the porous ZnO, **b** Barrett–Joyner–Halenda (BJH) pore size distribution plot from adsorption branch

microwave radiation [13]. In addition, [Bmim]BF_4 can decompose in the presence of transition metal salts with hydration water molecules when the temperature exceeds its boiling point, the reaction can be expressed as follows [13]:

$$BF_4{}^{-1}(IL) + H_2O \overset{\text{microwave}}{\rightarrow} BF_3 \cdot H_2O(IL) + F^{-1}(IL). \quad (1)$$

Generally, when the pH value is between 6 and 9, $Zn(OH)_2$ is obtained predominantly. But the ZnF^+ complexes will form in the presence of F^- under neutral or weak alkaline conditions, and the nucleation of Zn(OH)F occurs during further hydrolysis [19, 29]. A possible chemical mechanism can be expressed as follows:

$$Zn^{2+} + F^- \leftrightarrow ZnF^+ \quad (2)$$

$$ZnF^+ + OH^- \leftrightarrow Zn(OH)F \downarrow \quad (3)$$

The experiment results show that ionic liquid [Bmim]BF_4 plays a critical role in the formation of flower-like structure. In the reaction, supramolecular effects and solvent self-structuration of ionic liquid are important when it reacts with high concentration of zinc acetate [2]. The extended hydrogen-bonding and π–π stack interaction of the neighboring imidazolium rings make ionic liquids molecular recognition and self-assembly [30]. As "supramolecular" solvent, the self-assembled ability of ionic liquid ([Bmim]BF_4) has an important influence on the structural orientation in the reaction [31, 32]. Therefore, the flower-like morphology of Zn(OH)F is formed. The detailed formation mechanism needs to be further investigated.

ZnO is obtained after the calcination of Zn(OH)F at 400 °C, the chemical reaction takes place as follows: Zn(OH)F → ZnO + HF. During the thermal decomposition process, molecule-size pores generated when the HF molecules released from the flower-like particles. Meanwhile, small ZnO units formed during this process. With the temperature increasing, the small ZnO units assembled into nanoparticles and the molecule-size pores became nanopores. Because of the existence of nanopores, flower-like ZnO sample possesses a large BET surface area.

Conclusions

Novel flower-like Zn(OH)F has been successfully synthesized via microwave-assisted ionic liquid route. In addition, nanoporous ZnO is obtained after the heat treatment of Zn(OH)F, and the morphology is well retained. This method is fast and simple without using complex template. The ionic liquid [Bmim]BF_4 is used as the reactant and the template in the synthesis. It is expected that this method may be extended to the preparation of other inorganic materials.

Acknowledgments This work was supported by Natural Science Foundation of Jiangsu Province (BK2006195), Doctor Innovation Funds of Jiangsu Province (BCXJ06-13), and National Natural Science Foundation of China (50502020, 50701024).

References

1. Y. Liu, M.J. Wang, J. Li, Z.Y. Li, P. He, H.T. Liu, J.H. Li, Chem. Commun. 1778–1780 (2005). doi:10.1039/b417680d
2. M. Antonietti, D.B. Kuang, B. Smarsly, Z. Yong, Angew. Chem. Int. Ed. **43**, 4988–4992 (2004). doi:10.1002/anie.200460091
3. A. Taubert, Z. Li, Dalton Trans. 723–727 (2007). doi:10.1039/b616593a
4. Y. Jiang, Y.J. Zhu, G.F. Cheng, Cryst. Growth Des. **6**, 2174–2176 (2006). doi:10.1021/cg060219a
5. A.B. Panda, G. Glaspell, M.S. El-Shall, J. Am. Chem. Soc. **130**, 4203–4203 (2008)
6. L. Zhang, Y.J. Zhu, S.W. Cao, Chem. Lett. **37**, 1002–1003 (2008). doi:10.1246/cl.2008.1002
7. T. Suprabha, H.G. Roy, J. Thomas, K.P. Kumar, S. Mathew, Nanoscale Res. Lett. **4**, 144–152 (2009). doi:10.1007/s11671-008-9214-5
8. Z.Y. Lai, G.L. Xu, Z. Yalin, Nanoscale Res. Lett. **2**, 40–43 (2007). doi:10.1007/s11671-006-9027-3
9. D.K. Bhat, Nanoscale Res. Lett. **3**, 31–35 (2008). doi:10.1007/s11671-007-9110-4
10. J. Wang, J.M. Cao, B.Q. Fang, P. Lu, S.G. Deng, H.Y. Wang, Mater. Lett. **59**, 1405–1408 (2005). doi:10.1016/j.matlet.2004.11.062
11. K.L. Ding, Z.J. Miao, Z.M. Liu, Z.F. Zhang, B.X. Han, G.M. An, S.D. Miao, Y. Xie, J. Am. Chem. Soc. **129**, 6362–6363 (2007). doi:10.1021/ja070809c
12. G. Buhler, D. Tholmann, C. Feldmann, Adv. Mater. **19**, 2224–2227 (2007). doi:10.1002/adma.200602102

13. D.S. Jacob, L. Bitton, J. Grinblat, I. Felner, Y. Koltypin, A. Gedanken, Chem. Mater. **18**, 3162–3168 (2006). doi:10.1021/cm060782g
14. Y.P. Xu, Z.J. Tian, S.J. Wang, Y. Hu, L. Wang, B.C. Wang, Y.C. Ma, L. Hou, J.Y. Yu, L.W. Lin, Angew. Chem. Int. Ed. **45**, 3965–3970 (2006). doi:10.1002/anie.200600054
15. Y.J. Zhu, W.W. Wang, R.J. Qi, X.L. Hu, Angew. Chem. Int. Ed. **43**, 1410–1414 (2004). doi:10.1002/anie.200353101
16. L.X. Yang, Y.J. Zhu, W.W. Wang, H. Tong, M.L. Ruan, J. Phys. Chem. B **110**, 6609–6614 (2006). doi:10.1021/jp0569739
17. C. Xu, H. Luo, W.D. Liu, T.K. Ying, Ceram. Int. **35**, 917–919 (2009). doi:10.1016/j.ceramint.2008.03.002
18. J.M. Cao, J. Wang, B.Q. Fang, X. Chang, M.B. Zheng, H.Y. Wang, Chem. Lett. **33**, 1332–1333 (2004). doi:10.1246/cl.2004.1332
19. N. Saito, H. Haneda, W.S. Seo, K. Koumoto, Langmuir **17**, 1461–1469 (2001)
20. Q.L. Huang, M. Wang, H.X. Zhong, X.T. Chen, Z.L. Xue, X.Z. Yout, Cryst. Growth Des. **8**, 1412–1417 (2008). doi:10.1021/cg070539+
21. M. Mo, J.C. Yu, L.Z. Zhang, S.K.A. Li, Adv. Mater. **17**, 756–760 (2005). doi:10.1002/adma.200401477
22. H.D. Yu, Z.P. Zhang, M.Y. Han, X.T. Hao, F.R. Zhu, J. Am. Chem. Soc. **127**, 2378–2379 (2005). doi:10.1021/ja043121y
23. P. Li, Y. Wei, H. Liu, X.K. Wang, Chem. Commun. 2856–2857 (2004). doi:10.1039/b409425e
24. F. Xu, P. Zhang, A. Navrotsky, Z.Y. Yuan, T.Z. Ren, M. Halasa, B.L. Su, Chem. Mater. **19**, 5680–5686 (2007). doi:10.1021/cm071190g
25. J.B. Liang, S. Bai, Y.S. Zhang, M. Li, W.C. Yu, Y.T. Qian, J. Phys. Chem. C **111**, 1113–1118 (2007). doi:10.1021/jp0662808
26. Z.H. Li, A. Gessner, J.P. Richters, J. Kalden, T. Voss, C. Kubel, A. Taubert, Adv. Mater. **20**, 1–7 (2008). doi:10.1002/adma.200700935
27. B. Reeja-Jayan, E. De la Rosa, S. Sepulveda-Guzman, R.A. Rodriguez, M.J. Yacaman, J. Phys. Chem. C **112**, 240–246 (2008). doi:10.1021/jp0765704
28. C.X. Shan, Z. Liu, Z.Z. Zhang, D.Z. Shen, S.K. Hark, J. Phys. Chem. B **110**, 11176–11179 (2006). doi:10.1021/jp0600514
29. S. Yamabi, H. Imai, J. Mater. Chem. **12**, 3773–3778 (2002). doi:10.1039/b205384c
30. Y. Zhou, J.H. Schattka, M. Antonietti, Nano Lett. **4**, 477–481 (2004). doi:10.1021/cm034442w
31. W.J. Zheng, X.D. Liu, Z.Y. Yan, L.J. Zhu, ACS Nano **3**, 115–122 (2009). doi:10.1021/nn800713w
32. Z.J. Yang, J.K. Song, M.B. Zheng, S.T. Liao, H.Q. Chen, G.B. Ji, H.Y. Wang, J.M. Cao, Acta Chim. Sin. **66**, 2558–2562 (2008)